IOP Conf. Series: Journal of Physics: Conf. Series **871** (2017) 012094 doi:10.1088/1742-6596/871/1/012094

Numerical analysis of fundamental characteristics of superconducting magnetic bearings for a polarization modulator

Yusuke Terachi[1], Yutaka Terao[1], Hiroyuki Ohsaki[1], Yuki Sakurai[2], Tomotake Matsumura[2], Hajime Sugai[2], Shin Utsunomiya[2], Hirokazu Kataza[3] and Ryo Yamamoto[3]

[1]Graduate School of Frontier Sciences, The University of Tokyo, 5-1-5 Kashiwanoha, Kashiwa, Chiba 277-8561, Japan
[2]Kavli Institute for the Physics and Mathematics of the Universe (WPI), The University of Tokyo Institutes for Advanced Study, The University of Tokyo, 5-1-5 Kashiwanoha, Kashiwa, Chiba 277-8583, Japan
[3]Japan Aerospace Exploration Agency, Institute of Space and Astronautical Science (ISAS), 3-1-1 Yoshinodai, Chuo-ku, Sagamihara, Kanagawa 252-5210, Japan

E-mail: ohsaki@k.u-tokyo.ac.jp

Abstract. We have carried out numerical analysis of mechanical properties of a superconducting magnetic bearing (SMB). A contactless bearing operating at below 10 K with low rotational energy loss is an attractive feature to be used as a rotational mechanism of a polarization modulator for a cosmic microwave background experiment. In such application, a rotor diameter of about 400 mm forces us to employ a segmented magnet. As a result, there is inevitable spatial gap between the segments. In order to understand the path towards the design optimizations, 2D and 3D FEM analyses were carried out to examine fundamental characteristics of the SMBs for a polarization modulator. Two axial flux type SMBs were dealt with in the analysis: (a) the SMB with axially magnetized permanent magnets (PMs), and (b) the SMB with radially magnetized PMs and steel components for magnetic flux paths. Magnetic flux lines and density distributions, electromagnetic force characteristics, spring constants, etc. were compared among some variations of the SMBs. From the numerical analysis results, it is discussed what type, configuration and design of SMBs are more suitable for a polarization modulator.

1. Introduction

The measurement of the cosmic microwave background (CMB) has provided rich information about the physics of early universe [1, 2]. With a rapid progress in various cosmological observations, the experimental probe for the cosmic inflation is identified as one of the highest priorities in the field of cosmology. The corresponding technological improvements toward the high sensitivity measurements are in high demand. One of the key instruments to achieve this science goal is to employ a polarization modulator. The polarization modulator is an instrument to modulate incident linearly-polarized radiation. It consists of a continuously-rotating optical element, called a half-wave plate (HWP), and a rotational mechanism with a bearing. One requirement that makes this observational instrument challenging to


Content from this work may be used under the terms of the Creative Commons Attribution 3.0 licence. Any further distribution of this work must maintain attribution to the author(s) and the title of the work, journal citation and DOI.
Published under licence by IOP Publishing Ltd

implement is to cool an HWP to below 10 K during observations. Thus, the entire continuously-rotating system must operate at this temperature range. Thus, a conventional mechanical bearing is unsuitable due to the mechanical friction and the resultant heat dissipation.

A superconducting magnetic bearing (SMB) is a contactless bearing, which consists of an array of high temperature superconducting (HTS) bulk tiles and a permanent magnet (PM). Due to its nature of a levitation-based bearing, we identify this bearing to be an attractive candidate for a cryogenically continuously-rotating bearing for the CMB polarization modulator.

An SMB provides nearly but not perfectly frictionless rotation. This is due to a magnetic interaction between a rotor and a stator. The source of friction is originated from the magnetic field inhomogeneity of a rotor magnet [3, 4]. As the rotor spins, this spatial magnetic field inhomogeneity causes a time varying magnetic field for the stator, and a hysteresis and eddy current loss results in friction [5]. The energy loss is eventually dissipated as heat. The diameter of a rotor magnet is determined from the size of HWP, and thus the expected diameter is about 400 mm for CMB observations [6]. This forces us to use a segmented magnet to form a large ring, and the imperfection of a segment rotor magnetization and a fabrication error become a source of a magnetic field inhomogeneity. In order to minimize the heat dissipation to a cryogenic temperature stage from this rotational mechanism, one can explore the design parameters of the SMB, such as the SMB configuration, the rotor magnet geometry, and the levitation height. The magnetic field inhomogeneity is one of the key figure-of-merits, but we also study the stiffness as a figure-of-merit since the expected rotor mass including an optical element amounts about 30 kg.

In this paper, we present the numerical study for design parameter tradeoffs of SMB system for use in a CMB polarization modulator. We show a comparison of the magnetic field inhomogeneities for two segmented-rotor configurations: an axially-magnetized rotor magnet and a radially-magnetized rotor magnet. We also compute the spring constant for the axially-magnetized rotor magnet. Finally, we discuss the applicability of this technology for the polarization modulator as well as room for the optimization in an SMB design.

2. Superconducting magnetic bearing

Figure 1 shows a configuration of our SMB composed of a PM ring and bulk HTS tiles. There are two types of PM arrangements in the rotor, axially magnetized PMs and radially magnetized PMs as shown in figure 2 and 3, respectively. In both PM configurations, an assembled magnet has a gap between the segmented magnets inevitably. This gap results the magnetic field inhomogeneity. In addition to this effect, the ideal magnetization for the radial configuration is to magnetize the PM piece radially. In reality this is difficult to fabricate and we are forced to employ an arc-shaped PM piece that is magnetized in parallel instead of radially. This becomes another source of magnetic field inhomogeneity. The flux density variation needs to be reduced because it becomes a source of energy loss during rotation. We have considered following options to suppress the magnetic inhomogeneity of a segmented rotor magnet. For axially magnetized PMs, the insert of a single-piece of steel plate just below the PMs is effective to reduce the flux density variation [7], but it reduces also the amplitude of flux density. In this analysis, no addition of steel components was considered. As a part of effort to minimize the magnetic field inhomogeneity, the PMs are divided into two vertical stacks. Each are placed with a shift angle of $180/n$ between the upper and lower PM arrangements, where n is the number of PM segments. For a radially magnetized PM, steel pieces are placed on both the inner and outer sides of the PMs as shown in figure 3. The steel component is effective to reduce the flux density variation along the rotational direction. We address the quantitative assessment of these options numerically.

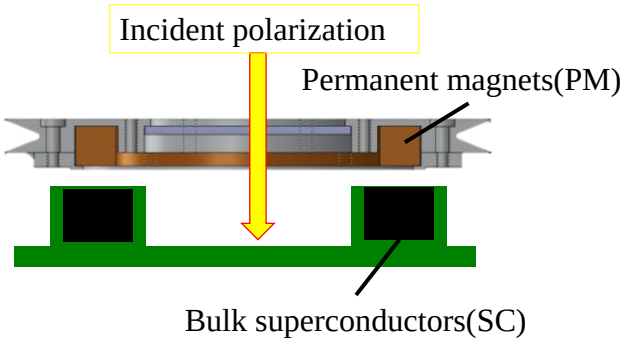

Figure 1. Superconducting magnetic bearing composed of PMs and bulk superconductors.

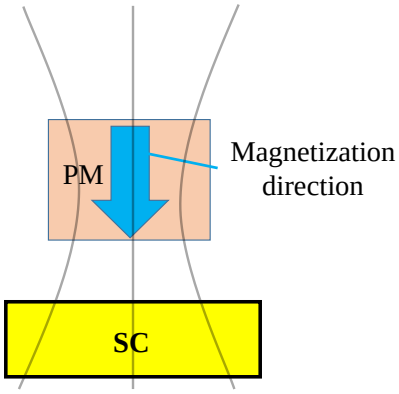

Figure 2. SMB with an axially magnetized PM ring.

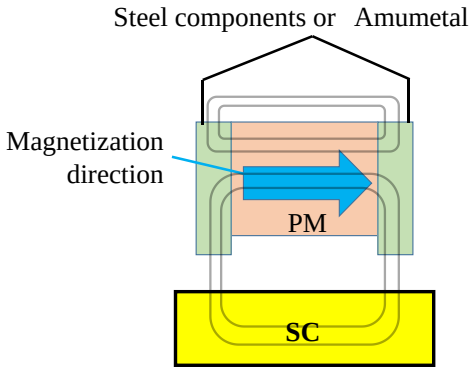

Figure 3. SMB with a radially magnetized PM ring and steel components.

3. Analysis models and conditions

3.1. Fundamental parameters of the SMB

Finite element analysis (FEA) was carried out using a commercial software, COMSOL Multiphysics, to examine the magnetic flux density distribution and the spring constant of the SMBs. Figure 4 shows a SMB model and its basic geometric parameters used in the FEA. Table 1 gives characteristic and geometric parameters of the PMs. The magnetic field of PMs can vary as a function of temperature [8], and we did not take into account this effect in the analysis.

A PM ring is divided into arc-shaped PM components. In the actual fabrication of the PM ring, a small mechanical gap cannot be avoided between adjacent PM components. Here the PM gap of 1 mm is assumed. In the analysis of SMBs, which have radially magnetized PMs with steel magnetic flux paths, the steel pieces with h_m ($> h_{PM}$) in height and w_m in width are placed on both the inner and outer side of the PMs. Here, h_m is set to 18 mm and w_m is 1 mm in all cases. The top surfaces of the PMs and the steel pieces are arranged to become a flat surface as shown in figure 3.

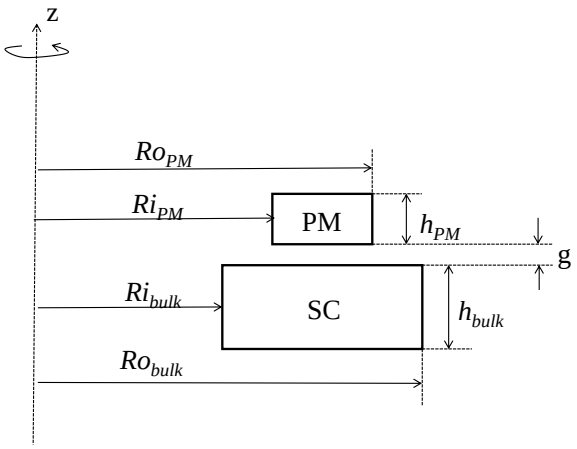

Figure 4. Arrangement of the permanent magnets and the bulk superconductors for FEM analysis.

Table 1. Parameters of permanent magnets.

Parameters	Values
Residual magnetic flux density B_r (T)	1.1
Inner radius Ri_{PM} (mm)	200
Outer radius Ro_{PM} (mm)	216
Height h_{PM} (mm)	16

3.2. Analysis of static spring constants

An axisymmetric FEA of magnetic fields was carried out to examine the magnetic spring constant of the SMB shown in figure 2 and 3. A gap between adjacent PMs was not considered and a radial magnetization of the PMs was assumed. A precise estimation of the magnetic spring constant would require the investigation of dynamic characteristics of the SMB with its superconducting properties such as an *E-J* relation taken into account. However, an approximate analysis based on a simple SMB model was adopted as the first step of the study. Namely, static spring constants were calculated using a magnetic flux frozen model, where an infinite critical current density was assumed. The analysis procedure is as follows:

i) Calculate the magnetic field in the analysis region including the SMB model without the bulk superconductor for a given initial levitation gap; g_0 between the bulk superconductor and the PM. The region of the bulk superconductor is set to air. Magnetic vector potentials in the analysis region are obtained.
ii) Obtain the magnetic vector potentials on the surface of the bulk superconductor region. They are used as one of boundary conditions for the next analysis. This boundary condition corresponds to the magnetic flux frozen state of the bulk superconductor with an infinite critical current density approximation.
iii) The above boundary condition is applied to the surface of the bulk superconductor. A small vertical displacement; Δg is given to the levitated body by changing the gap between the bulk superconductor and the PM. Moreover, calculate the magnetic field in the analysis region.
iv) Calculate the magnetic force acting on the levitated body by the nodal force method.
v) From the obtained magnetic forces for the gaps, g_0 and $g_0+\Delta g$, the spring constant can be estimated.

By changing the initial levitation gap, the relation between the static spring constant and the gap can be obtained. The FEAs were carried out for the SMBs with the axially magnetized PMs and with the radially magnetized PMs. The gap was changed in the range from 2 to 5 mm.

3.3. Analysis of magnetic field inhomogeneity

Three-dimensional FEM analysis was carried out to investigate the distribution of the axial magnetic flux density along a coaxial circular path on the upper surface of bulk superconductor. It was assumed here that the axial flux density distribution could be used as an evaluation parameter of the rotational loss of the SMBs. In the SMB with the axially magnetized PMs the circular path was placed in the middle of the top surface of bulk superconductor as shown in figure 5 while in the SMB with the radially magnetized PMs and the steel magnetic circuit the circular paths are placed on the bulk superconductor surface right below the steel pieces, as shown in figure 6. The radius of the circular path is 208 mm in the case of axial magnetization type. And the radii of the inner and outer circular paths are 199.5 mm and 216.5 mm, respectively, in the case of radial magnetization type. The levitation gap, g, is defined as the minimum distance between the bulk superconductor and the levitated component (the axially magnetized PMs or the steel pieces). The levitation gap was set to 5 mm in the analysis. The distribution of circumferential B_z of the axial magnetization type (n=8) is shown in figure 5. In addition, the distribution of circumferential B_z of the radial magnetization type (16 segments) is shown in Fig. 6. A magnetic flux density variation; ΔB is defined as $B_{max} - B_{min}$ along the circular path. We employ $\Delta B/B$ as a figure-of-merit of the magnetic field inhomogeneity.

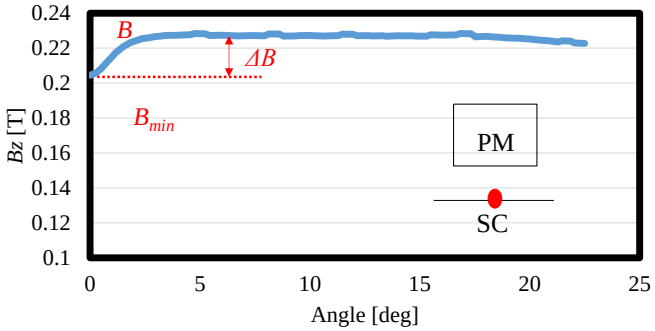

Figure 5. Magnetic flux density distribution generated by the axially magnetized PMs.

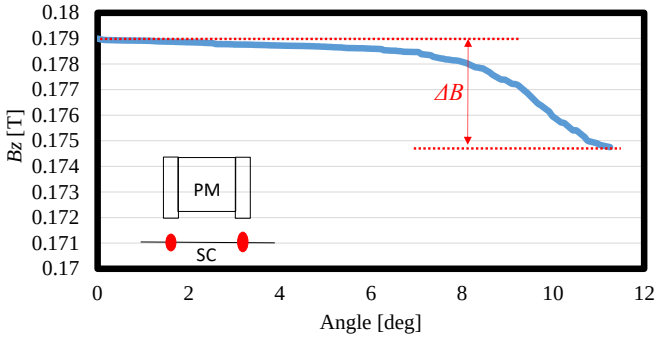

Figure 6. Magnetic flux density distribution generated by the radially magnetized PMs with steel components.

4. Analysis results

4.1. Spring characteristics

Static spring constants of the two types of SMBs were analyzed using the magnetic flux frozen approximation for the bulk superconductor. Figure 7 shows the results of the analysis for the levitation gap range from 2 to 5 mm. The spring constant is on the order of 10^5 N/m and decreases with an increase in the gap. The SMB with PMs having the axial magnetization has a larger spring constant than that with PMs having the radial magnetization and the steel magnetic circuit. An SMB for a smooth and ultra-low loss rotation of the HWP used in CMB polarization experiments is required to have a spring constant of at least a few 10^5 N/m and, if possible, as large as 10^6 N/m. The results shown in figure 7 satisfy the minimum requirement, but a design improvement will be needed for a better SMB performance. The approximation of the analysis has to be carefully considered again. The results were obtained on the approximation of the static analysis and the magnetic flux frozen model. A dynamic motion of the levitated body would generate larger currents in the superconductor than a static case if we consider the *E-J* characteristics of the superconductors with critical state models [9, 10]. Therefore, the static analysis gives us a smaller spring constant. On the other hand, the magnetic flux frozen model assumes an infinite critical current of the superconductor, and gives us a larger spring constant. Therefore, we consider that the static analysis and the magnetic flux frozen model would be an acceptable approximation for the estimation of the spring constant of the SMB in the first step of the study.

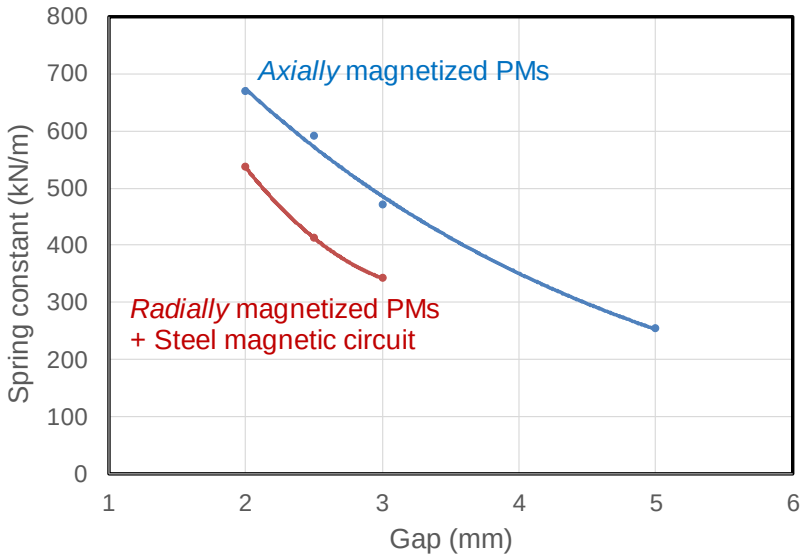

Figure 7. Dependence of the static spring constant on the levitation gap for the two types of SMBs. The SMB with axially magnetize PMs, and the SMB with radially magnetized PMs and the steel magnetic circuit.

4.2. Evaluation of $\Delta B/B$

In the case of the radial magnetization type, the magnetic field, *B,* vs the number of divisions, *n,* is shown in figure 8. The magnetic field, *B,* reaches the peak when *n* is between 8 and 16 due to a predominant effect of the increase in the radial component of magnetic flux density. However, when *n* increased continuously, *B* decreases because of the decrease in the volume of PMs fractionally with respect to the gap volume.

The magnetic field inhomogeneity, $\Delta B/B$, keeps decreasing as n increases as shown in figure 8. The design goal of the magnetic field inhomogeneity is $\Delta B/B < 0.01$. The magnetic field inhomogeneity, $\Delta B/B$, is found to be small enough to meet the requirement when n is over about 50 divisions as shown in figure 9.

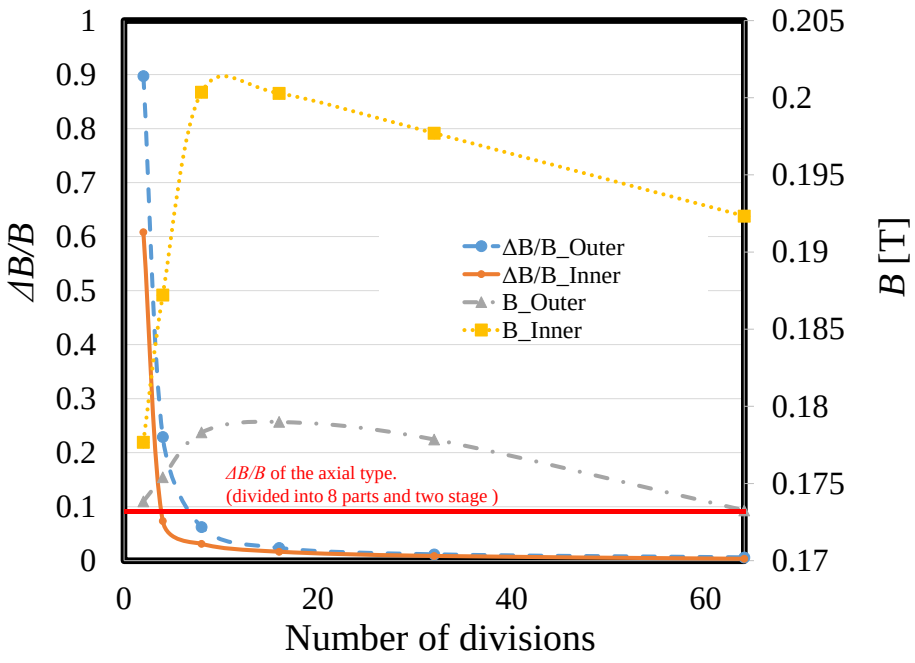

Figure 8. $\Delta B/B$ and B vs number of divisions.

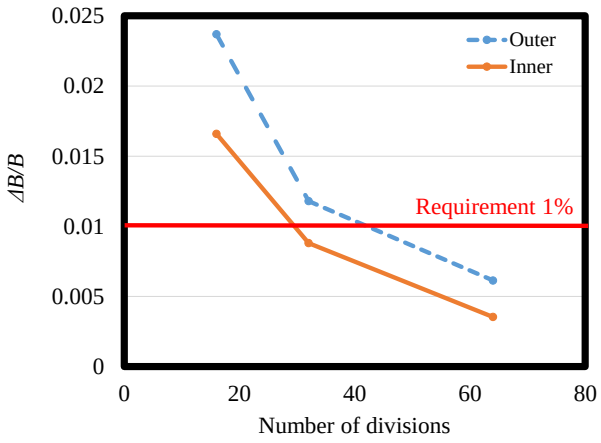

Figure 9. Vertically enlarged version of $\Delta B/B$ vs number of divisions.

5. Conclusions

We conducted the numerical studies to explore the design parameters of SMB using the FEA. We conclude that we did not find no-go result for the SMB to use for the polarization modulator in the CMB experiment even where a rotor diameter is about 400 mm and the rotor PM has to be assembled by a collection of segment PMs. We showed the results of the spring constant for two different rotor PM configurations, the segmented rotor magnet in the axially magnetized and the pseudo-radially magnetized. By employing a magnetic frozen flux approximation, we obtained the spring constants in range of 10^5 N/m. This is well within the range of need for the polarization modulator, and thus this result drive us to move to the detailed implementation of the physical model, including the properties of the superconductor and the dynamical effect, to derive the spring constant. The magnetic field inhomogeneity, $\Delta B/B$, in the axial magnetization of PM was about 10%. However, in the radial magnetization of PM, we demonstrated to suppress the $\Delta B/B$ as low as 1 %, that is the requirement value. This study guides us to construct a rotor magnet as well as investigate the further analyses, including computing the rotational loss with superconducting characteristics.

Acknowledgement

This work was supported by MEXT KAKENHI Grant Numbers JP15H05441 and JSPS Core-to-Core Program, A. Advanced Research Networks. This work was also supported by World Premier International Research Center Initiative (WPI), MEXT, Japan.

References

[1] Sato K 1981 First-order phase transition of a vacuum and the expansion of the Universe *Monthly Notices of the Royal Astronomical Society Vol* 195 no 3 p 467
[2] Guth A H 1981 Inflationary universe: A possible solution to the horizon and flatness problems *Physical Review D Vol 23 no* 2 p 347
[3] Kaneko H, Miyagawa Y, Takahata R and Ueyama, H 1999 Rotation loss characteristics of superconducting magnetic bearings *TEION KOGAKU (Journal of Cryogenics and Superconductivity Society of Japan) Vol* 34 *no* 11 p 678.
[4] Shimizu R., Demachi K and Miya K 1999 Development evaluation method of AC loss in high temperature superconductor *Presented in 11th Symposium on Electromagnetics and Dynamics*
[5] Hull J R, Mulcahy T M, Uherka K L and Abboud R G 1995 Low rotational drag in high-temperature superconducting bearings *IEEE Trans. on Appl. Supercond. Vol* 5 *no 2* p 626
[6] Sakurai Y, Matsumura T, Sugai H, Katayama N, Hiroyuki Ohsaki H, Terao Y, Terachi Y, Kataza H, Utsunomiya S, Yamamoto R 2016 Vibrational characteristics of a superconducting magnetic bearing employed for a prototype polarization modulator *Preprint* ISS2016/AP2-5
[7] Higasa H, Ishikawa F, Kawauchi N, Yokoyama S, Nakamura S, Imaizumi H and Ito N 1994 Experiment of a 100Wh-Class Power Storage System using High-Tc Superconducting Magnetic Bearing *Advances in Superconductivity VI* (Springer Japan) p 1249
[8] Hara T, Tanaka T, Kitamura H, Bizen T, Maréchal X, Seike T, Kohda T and Matsuura Y 2004 Cryogenic permanent magnet undulators *Physical Review Special Topics-Accelerators and Beams Vol* 7 *no* 5 050702.
[9] Bean C P 1964 Magnetization of high-field superconductors *Reviews of Modern Physics Vol* 36 *no* 1 p 31
[10] Kim Y B, Hempstead C F and Strnad A R 1962 Critical persistent currents in hard superconductors *Physical Review Lett. Vol* 9 *no* 7 p 306.